The International Journal of Engineering and Science (IJES)
|| Volume || 14 || Issue 8 || August || Pages || PP 69-77 || 2025 ||
ISSN (e): 2319 – 1813 ISSN (p): 2319 – 1805

# Error Vector Magnitude Analysis on Digital Wireless Signal Reflection from NaCl and Alcohol

Koyu Chinen[1] and Ichiko Kinjo[2]
[1]*GLEX, Yokohama, Japan*
[2]*National Institute of Technology, Okinawa College, Okinawa, Japan*
*Corresponding Author: Koyu Chinen*

***ABSTRACT***
*High-frequency signal reflection characteristics of aqueous NaCl and alcohol solutions were investigated using digital wireless signals of QPSK, 16-QAM, and 64-QAM modulation formats. A vector-signal-generator sent the signals through an SMA probe to aqueous solutions, and a vector-signal-analyzer analyzed the reflected signals through a beam splitter. The concentration of the NaCl solution varied from 0.001 to 3 mol/L, the alcohol concentration ranged from 5 to 99.5%, and the reflected S-parameter ($S_11$) was measured from 1 to 4500 MHz using a vector-network analyzer. A specific carrier frequency of 3300 MHz was determined due to the minimum value of $|S_{11}|$. Error vector magnitude (EVM), constellation, and signal power (Pwr) of reflected signals were measured. The aqueous NaCl solution has a considerable Pwr value due to the rotation and vibration of the polar molecule $H_2O$ and cluster, even at high solute concentrations. In contrast, the aqueous alcohol solution shows a maximum value of EVM and then decreases due to the decrease in $H_2O$ amount at high alcohol concentrations. The EVM values depend on the magnitude of $|S_{11}|$ and Pwr due to the impedance change caused by the concentration of the polarized molecule $H_2O$, since the aqueous solutions are considered a passive equivalent circuit.*

***KEYWORDS;*** *NaCl solution; alcohol solution; polar H2O; QAM-OFDM; S-parameter; EVM; impedance; Smith chart*

Date of Submission: 10-08-2025 Date of acceptance: 23-08-2025

## I. INTRODUCTION

Electrical impedance spectroscopy (EIS) has been used to measure the impedance and synthesize the electrical equivalent circuits of biomaterials and chemical materials, such as food [1], plants [2-4], NaCl solutions [5, 6], and alcohols [7, 8]. Generally, the EIS method uses a low-frequency signal due to impedance mismatch in the high-frequency range for the I-V measurement system. We have used an S-parameter measurement that allows high-frequency measurements to evaluate the impedance and properties of aqueous solutions [9], alcohols [10], plants [11], cell walls [12], and cell vacuoles [13], and to synthesize these equivalent circuits. The S-parameter measurement methods use sinusoidal and square-wave modulated signals.

Digital wireless signals have been used in wireless fidelity (Wi-Fi) and cellular communications in recent years. Digital wireless signals use quadrature amplitude modulation (QAM) and orthogonal frequency division multiplexing (OFDM) to modulate digital baseband signals at high speed and high density [14]. Digital wireless signals are suitable for high-speed and long-distance communications because they reduce multipath interference and correct the communication error rates. Analysis of the electrical properties of materials using digital wireless signals can yield new insights into the materials. Analysis of the reflection characteristics between digital wireless signals and materials is also essential to ensure the quality of digital wireless communications.

In this study, aqueous NaCl and alcohol (ethanol) solutions were chosen as representative examples of materials that reflect digital wireless signals. The aqueous NaCl solutions contain $Na^+$ and $Cl^-$ ions and polar water molecules, $H_2O$, and thus are highly similar to the composition and properties of biological and chemical materials. The alcohol solutions contain low-conductivity alcohols and polar water molecules, $H_2O$, and are very similar to the composition and properties of foods and drinking water. This study has first used multi-level QAM-OFDM digital wireless signals to investigate the relationship between aqueous solution concentration, S-parameters, reflected signal power, and error vector magnitude (EVM).

## II. EVM MEASUREMENTS FOR AQUEOUS SOLUTIONS USING DIGITAL WIRELESS SIGNAL

The signal reflection characteristics of high-frequency wireless signals in aqueous solutions were evaluated using a measurement system shown in Fig. 1. A vector network analyzer (VNA) [15] was used to measure the reflection coefficient ($S_{11}$) of the scattering parameter (S-parameter) in the 1 MHz to 4500 MHz frequency range. The EVM value was measured using a setup of a vector signal generator (VSG) [16] and analyzer (VSA) [17]. S-parameter measurements using the VNA and EVM measurements using the VSG-VSA were performed separately. The material under test (MUT) was an aqueous solution in a glass container (approximately 15 ml). A high-frequency signal transmitted from the instrument is input into the aqueous solution through a subminiature type-A (SMA) probe inserted into the aqueous solution. The VNA and VSA receive signals reflected from the solution. The digital wireless signal transmitted from VSG and reflected by the aqueous solution is transmitted to VSA through a signal splitter. The SMA probe consists of a central signal pin (gold-plated copper, 4 mm in length and 0.8 mm in diameter) surrounded by polytetrafluoroethylene (PTFE) and four ground pins (4 mm apart from the signal pin). A pseudo-random bit sequence (PRBS) baseband digital signal was modulated with QAM in four formats (BPSK, QPSK, 16-QAM, and 64-QAM), and each symbol was modulated by inverse fast Fourier transform (IFFT) to 256-OFDM subcarriers in a modulation bandwidth of 10 MHz. The digital wireless signal generated by the VSG was transmitted to the MUT and reflected and sent through a beam splitter to the VSA, where the received power (Pwr), EVM, spectrum, and symbol error were analyzed.

Although we investigated the relation between Pwr and $S_{11}$, in a usual transmission system, the Pwr and EVM are substantially related to the transmission coefficient, $S_{21}$, since $S_{11}$ is very low. Hence, in this experiment, we changed the $S_{11}$ to $S_{21}$in the measurement setup to investigate the relation between EVM, $S_{11}$, and Pwr.

Figure 2 shows the measured reflection coefficient |S11 | of the VNA for the solvent with no added solute (pure water). The impedance of pure water is closest to the characteristic impedance of the measurement system, 50 Ω, at 3300 MHz. Therefore, we investigated the reflection characteristics of digital wireless signals at 3300 MHz. The reflection coefficient $S_{11}$ of the S parameter is the ratio of the reflected voltage $V_r$ to the incident voltage $V_i$, expressed as $S_{11}$ (dB) = 20log ($V_r / V_i$ ).

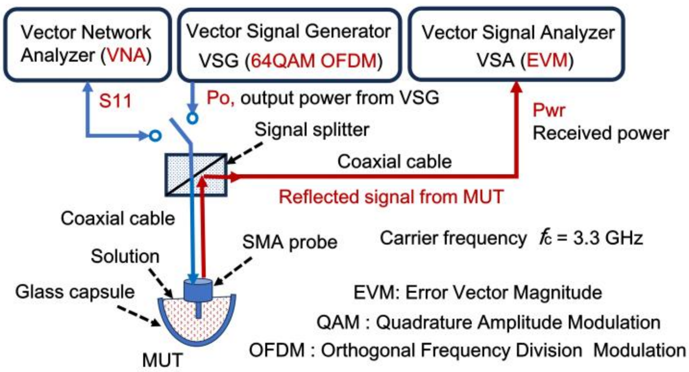


**Figure 1: A vector network analyzer (VNA) measures S-parameters $S_{11}$ by measuring reflected signals from aqueous solutions. Vector signal generator (VSG) and vector signal analyzer (VSA) measure error vector magnitude (EVM) and received power (Pwr) of digital wireless signals reflected from aqueous solutions and split by a beam splitter. A multipin SMA probe was used to measure the incidence and reflection of the RF signals in an aqueous solution.**

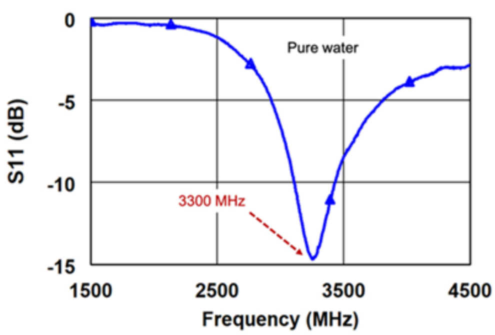


**Figure 2: S-parameter reflection coefficient, S11, was measured with MUT of pure water by vector network analyzer (VNA).**

## III. EVM MEASUREMENTS PRINCIPLE

EVM is a numerical value representing the average of the magnitude of the vector difference between the ideal symbol coordinates ($I_i$, $Q_i$) and the measured symbol coordinates ($I_m$, $Q_m$) in in-phase and quadrature-phase IQ coordinates, as shown in Fig. 3. The ratio of the root mean square (rms) of the sum of the ideal symbol coordinates ($I_{n,i}$, $Q_{n,i}$) of symbol n to the rms of the sum of the differences between the ideal symbol coordinates ($I_{n,i}$, $Q_{n,i}$) and the measured symbol coordinates ($I_{n,m}$, $Q_{n,m}$) is expressed by Eq. (1).

$$EVM_{n,rms} = \frac{\sqrt{\sum_{-n/2}^{n/2}\left[(I_{n,m} - I_{n,i})^2 + (Q_{n,m} - Q_{n,i})^2\right]}}{\sqrt{\sum_{-n/2}^{n/2}\left[{I_{n,i}}^2 + {Q_{n,i}}^2\right]}} \tag{1}$$

Hence, the EVM of symbol n is expressed by Eq. (2).

$$EVM = 20\log_{10} EVM_{n,rms} \tag{2}$$

$$P_{wr} \propto \sqrt{\sum_{-n/2}^{n/2}\left[{I_{n,i}}^2 + {Q_{n,i}}^2\right]} \tag{3}$$

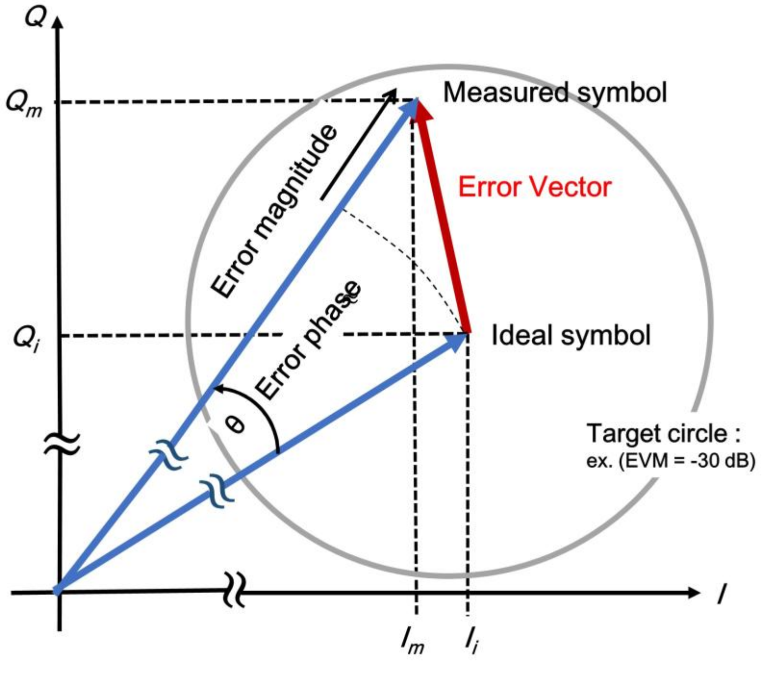


**Figure 3: Ideal symbol coordinates ($I_i$, $Q_i$) and measurement symbol coordinates ($I_m$, $Q_m$) are represented in *I* (in-phase) and *Q* (quadrature-phase) coordinates. The difference between the two points is the Error Vector**

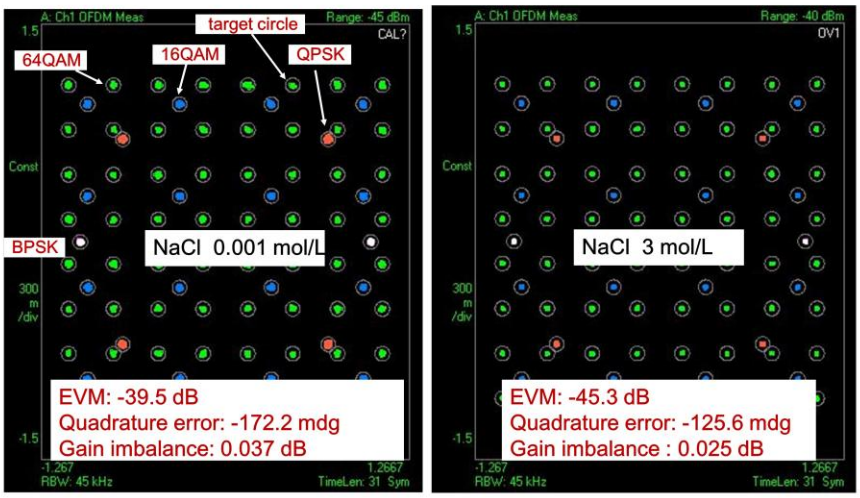


**Figure 4: The constellation of symbols was analyzed by VSA for reflected signals from aqueous solutions of different NaCl concentrations using digital wireless signals of four modulation formats (BPSK, QPSK, 16-QAM, 64-QAM).**

The digital wireless signal we used consists of four modulation formats: BPSK, QPSK, 16-QAM, and 64-QAM, with 2, 4, 16, and 64 symbols, respectively. Each symbol consists of PRBS baseband signals of 1, 2, 4, and 6 bits, respectively, and is mapped to IQ coordinates. Therefore, the number of symbols for each modulation format is represented by $2n$ ($n$ = 1, 2, 4, 6). The received Pwr at VSA is proportional to the sum of the ideal symbols as represented by Eq. (3). The digital wireless signals we used were modulated by four different formats: BPSK, QPSK, 16-QAM, and 64-QAM. The main data modulation formats were QPSK, 16-QAM, and 64-QAM, each with a symbol length of 10. Pwr and EVM of each modulation format were almost the same. Therefore, the values of Pwr and EVM in this report were measured using symbols with the 64-QAM modulation format [18].

## IV. EVM MEASUREMENTS FOR AQUARIUS NACL SOLUTIONS USING DIGITAL WIRELESS SIGNALS

Using digital wireless signals, we measured the EVM reflection characteristics of different NaCl molar concentrations. Figure 4 shows the measured values of EVM and Pwr, and the constellation of each symbol. In Fig. 4, the circle shown for each symbol is the target circle, and if the demodulated data of the symbol is within this circle, the EVM is less than -30 dB. When the concentration of the NaCl solution was as low as 0.001 mol/L, the EVM was -39.5 dB; when the NaCl concentration was as high as 3 mol/L, the EVM was -45.3 dB, about 6 dB less. The values of EVM and Pwr of the reflected signal from the NaCl solution measured at 3300 MHz are shown in Fig. 5 when the NaCl concentration in the solution was varied from 0.0001 mol/L to 3 mol/L. The EVM value decreased with NaCl concentration, and the Pwr value increased with NaCl concentration. The result is consistent with the theory that EVM is inversely proportional to Pwr and SNR, as represented in Eq. (1). The $S_{11}$ value is increased with the NaCl concentration, as shown in Fig. 6, and Pwr values showed almost the same characteristics. We investigated the cause of the increase in $S_{11}$ with NaCl concentration: $S_{11}$ was measured in the frequency range from 1 to 4500 MHz as the NaCl concentration was varied from 0.0001 mol/L to 3 mol/L. The measured $S_{11}$(complex number) was plotted on the admittance grid of a Smith chart, as shown in Fig. 7, using a Cadence AWR Design Environment software [19]. The origin S (0, 0) of the Smith chart is determined by $Z_0$ = 50 Ω and $Y_0$ = 0.02 S. The distance between the origin and the $S_{11}$ point at 3300 MHz on the curve for each NaCl concentration represents the reflection coefficient $|S_{11}|$. The dashed circle of equal radius represents the value of $S_{11}$ as a polar coordinate, and the value of $S_{11}$ at 3300 MHz increases with the NaCl concentration. The impedance (admittance) of the aqueous solution at 3300 MHz differs from 50 Ω (0.002 S) as the NaCl concentration increases. This impedance difference increases $S_{11}$ and Pwr. The frequency 3300 MHz is related to the rotation and vibration frequency of the polar molecule $H_2O$ and cluster. In addition, the SMA probe configuration determines the specific value of the resonant frequency of 3300 MHz since the polar molecular $H_2O$ and cluster have a wide range of resonant frequencies [20]. Therefore, the NaCl ion does not play a substantial role in the change in $S_{11}$.

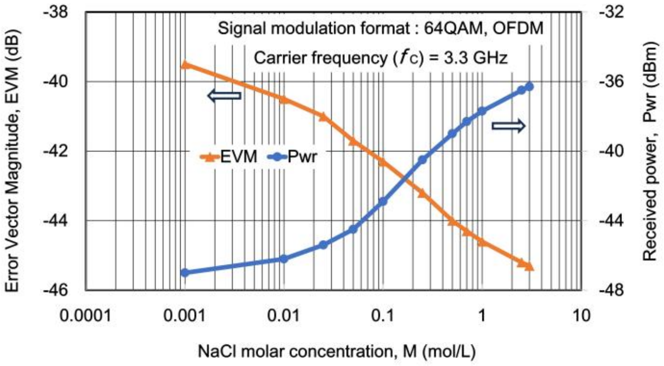


**Figure 5: Reflected signals from aqueous solutions in the NaCl concentration range 0.001 mol/L to 3 mol/L were measured by the vector signal analyzer (VSA) for error vector magnitude (EVM) and received power (Pwr).**

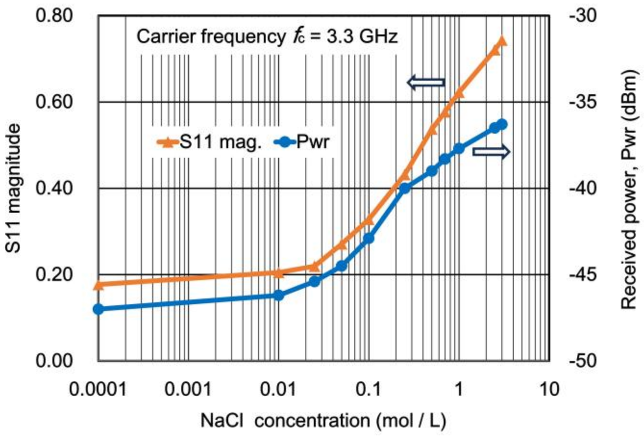


**Figure 6: Reflection coefficient, $S_{11}$, was measured at 3300 MHz using the VNA. Pwr was measured using the VSA for the reflected digital wireless signals from aqueous solutions in the NaCl concentration range of 0.001 mol/L to 3 mol/L.**

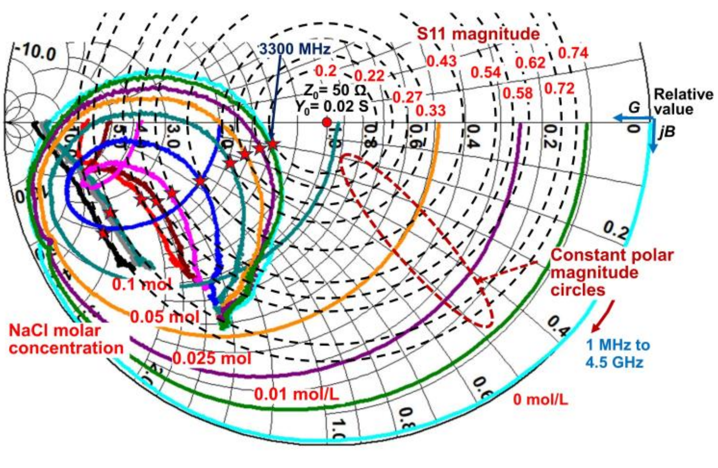


**Figure 7: S-parameter $S_{11}$ measurements result using high-frequency signals in the range of 1 MHz to 4500 MHz reflected from aqueous solutions in the NaCl concentration range of 0.001 mol/L to 3 mol/L, plotted on the admittance grid of a Smith chart. The intersections of the equal radius circles ($|S_{11}|$) of $S_{11}$ at 3300 MHz frequency are indicated by stars. The dashed circle of equal radius represents the value of $|S_{11}|$ as a polar coordinate.**

## V. EVM MEASUREMENTS FOR ALCOHOL SOLUTIONS BY REFLECTED DIGITAL WIRELESS SIGNALS

EVM reflection characteristics were evaluated for aqueous solutions with different alcohol (ethanol) concentrations. Figure 8 shows the EVM values and the constellation of each symbol. For a low alcohol concentration of 5%, the EVM was -41 dB, and for a high concentration of 50%, the EVM was -45 dB, about 4 dB lower.

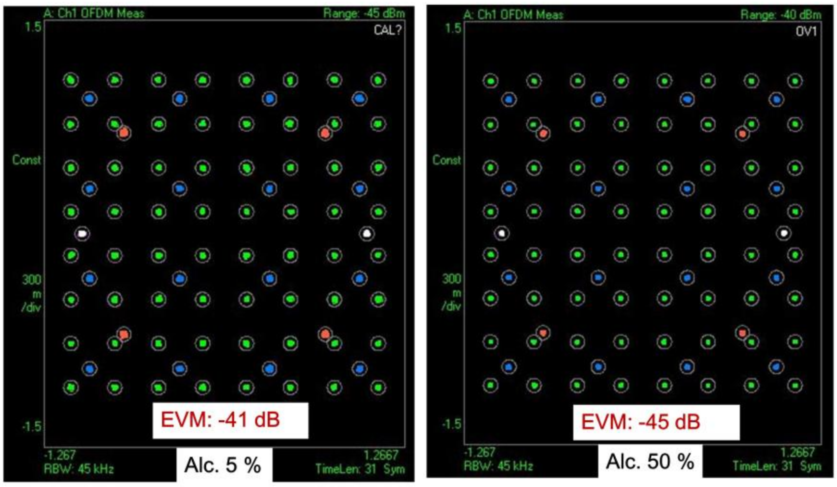


**Figure 8: The constellation of symbols was analyzed by VSA for reflected signals from aqueous solutions of different alcohol concentrations using digital wireless signals of four modulation formats (BPSK, QPSK, 16-QAM, 64-QAM).**

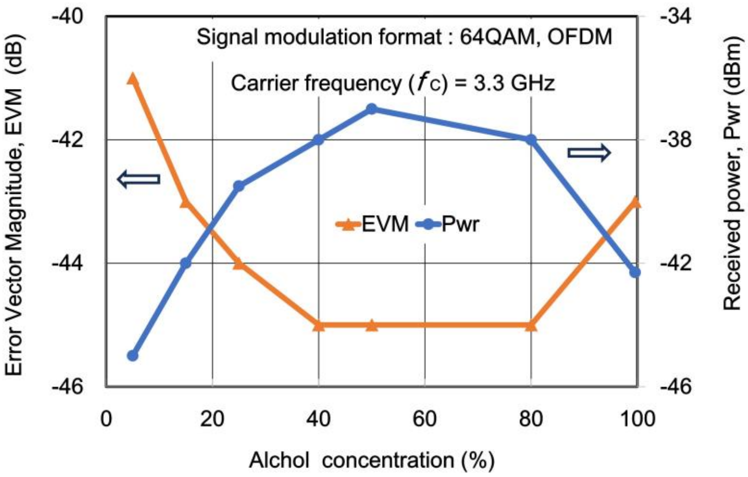


**Figure 9: EVM and Pwr were measured by VSA with reflected digital signals from aqueous solutions in the alcohol concentration range of 5 to 99.5%.**

The values of EVM and Pwr were measured with alcohol solutions at a frequency of 3300 MHz. The alcohol concentration was varied from 5 to 99.5%, as shown in Fig. 9. In the alcohol concentration range of 5 - 50%, the EVM decreased and Pwr increased with the concentration. However, when the concentration was increased to 50 - 95%, the EVM value increased, and Pwr decreased with the concentration.

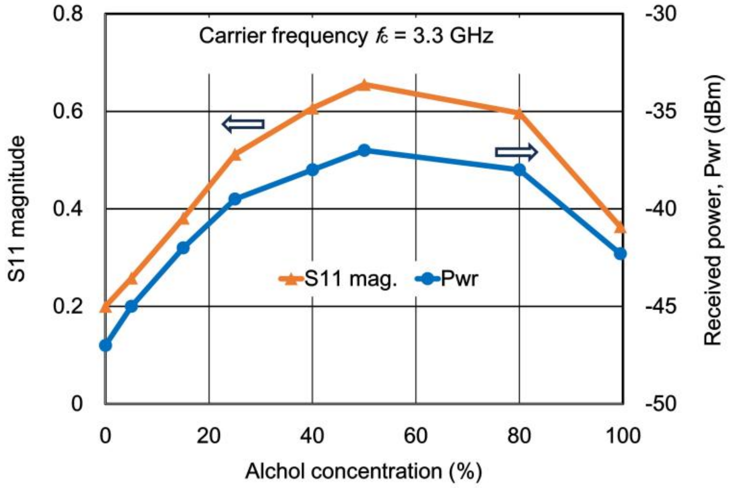


**Figure 10: Reflection coefficient, $S_{11}$, was measured with VNA at 3300 MHz, and Pwr was measured with VSA using reflected digital wireless signals from aqueous solutions, in the alcohol concentration range 0 to 99.5%.**

The $S_{11}$ value increased with the concentration in the 0 - 50% range and decreased in the 50 - 95% range, as shown in Fig.10. The Pwr value and the reflection coefficient $|S_{11}|$ showed almost the same characteristics. We investigated the cause of the change in the $S_{11}$ with alcohol (ethanol) concentration. The $S_{11}$ was measured in the frequency range from 1 to 4500 MHz as the alcohol concentration was varied from 0 to 95%. The measured $S_{11}$value was plotted on the admittance grid of a Smith chart, as shown in Fig. 11. The distance between the $S_{11}$ point at 3300 MHz and the Smith chart origin for each concentration represents the reflection coefficient $|S_{11}|$. The dashed circle of equal radius represents the value of $|S_{11}|$ as a polar coordinate. In the alcohol concentration range from 0 to 50 %, the $S_{11}$ value increased with increasing concentration. The impedance (admittance) difference at 3300 MHz increased with concentration.

In the concentration range of 50 - 95%, the opposite trajectory was observed, with a decrease in $S_{11}$. The $S_{11}$ value of isopropanol (IPA) was also examined for a reference, and the trajectory was similar to that of high alcohol concentrations. The relationship between EVM, Pwr, $S_{11}$, and solute concentration in the low alcohol concentration range of 5 - 50% showed similar changes to those in the low NaCl concentration range of 0.001 - 3 mol/L. The contribution of the polar molecule $H_2O$ is enormous in the low-content solutions. The admittance decreases for high alcohol concentrations from 50 to 99.5%, and the admittance also decreases for high NaCl concentrations of several mol/L or higher. This phenomenon is related to the rotation and vibration of the polar molecule $H_2O$ and its cluster.

In the case of high NaCl concentration, the amount of solvent $H_2O$ does not change. Hence, ionized atoms of $Na^+$ and $Cl^-$ and hydrated ions are frictional factors for $H_2O$ and cluster oscillation and rotation, but the admittance by $H_2O$ is relatively large. On the other hand, the amount of $H_2O$ decreases significantly in the high concentration of aqueous alcohol solution. In the case of an alcohol concentration of 99.5% and IPA, the role of the vibration and rotation due to polarized molecules $H_2O$ and cluster are significantly reduced. The polarity parameters P′ of IPA, ethanol, and $H_2O$ are 3.9, 4.3, and 10.2, respectively [21]. The difference in $S_{11}$ between IPA, ethanol, and $H_2O$ is due to these P′ values. The P′ value of $H_2O$ is significantly higher than that of the other molecules. The reflection characteristics of digital wireless signals from aqueous solutions highly depend on the amount of polarized molecular $H_2O$ and clusters.

In this article, we discuss the relationship between EVM and Pwr, because the $S_{11}$ value is a dominant factor in determining the EVM. However, we measured a significant difference in quadrature error between low and high EVM, as shown in Fig. 4. Since the equivalent circuit of the aqueous is a passive circuit, it is not easy to analyze the quadrature error using the passive circuit. The relation between EVM and quadra error will be analyzed and published elsewhere using a polar molecule motion equation.

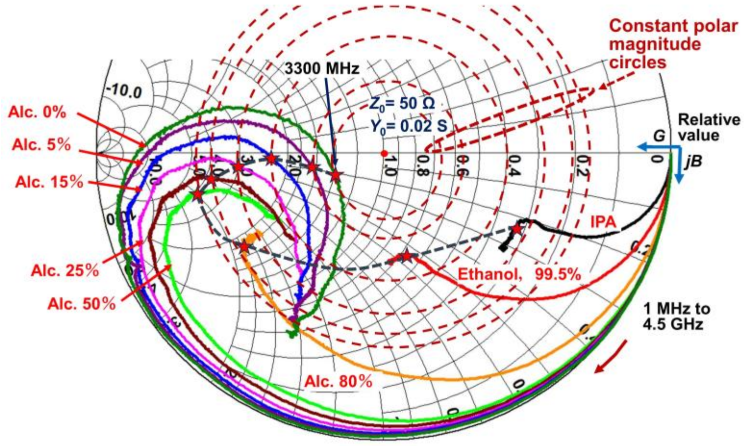


**Figure 11: S-parameter, $S_{11}$, measurements using high-frequency signals in the range of 1 to 4500 MHz reflected from aqueous solutions in the alcohol concentration range of 0 to 99.5%, plotted on the admittance grid of a Smith chart. The intersections of the equal radius circles of $|S_{11}|$ at 3300 MHz frequency are indicated by stars. The dashed circle of equal radius represents the value of $S_{11}$ as a polar coordinate. The measurement result of isopropanol IPA is plotted for reference.**

## VI. CONCLUSION

S-parameters, EVM, and Pwr of aqueous NaCl and alcohol (ethanol) solutions were measured using a network analyzer VNA and a digital wireless signal transmitter/receiver (VSG - VSA). The NaCl concentration varied from 0.001 mol/L to 3 mol/L, and the alcohol concentration ranged from 3 to 95.5%. The resonance frequency of 3300 MHz was used as the carrier frequency of the digital wireless signal. The resonant frequency is believed to be determined by the rotation and vibration of the polar water molecule $H_2O$ and the cluster, as well as the structure of the SMA probe. The digital wireless signal was modulated by four different formats of quadrature phase amplitude modulation (BPSK, QPSK, 16-QAM, 64-QAM) of the PRBS baseband signal. Each symbol is mapped to IQ coordinates and modulated with 256 OFDM subcarriers, and after D/A conversion, the signal is transmitted from the VSG. The SMA probe injected the digital radio signal into the aqueous solution. The signal reflected from the aqueous solution was transmitted to VSA through a beam splitter. Pwr and EVM were measured at the VSA.

As the concentration of NaCl and alcohol molecules in the solution increases, the impedance (admittance) of the solution at 3300 MHz differs from the reference impedance of 50 Ω (0.02 S), and the reflection coefficient S11 increases, resulting in an increase in Pwr and a decrease in EVM. The aqueous solution is considered an equivalent electrical passive circuit element, and an increase in the reflection coefficient $|S_{11}|$ does not increase the error vector, so the EVM value decreases.

Since $S_{11}$ of the aqueous solution depends on the resonance caused by the rotation and vibration of the polar water molecule $H_2O$ and cluster, $S_{11}$ and Pwr become smaller as the concentration of $H_2O$ increases. The reflection characteristics of digital wireless signals from aqueous solutions highly depend on the amount of polarized molecular $H_2O$. The EVM value increases the symbol-clock error in the wireless signal transmission system. This study also clarified the relationship between the reflection of digital wireless signals, chemical materials, and biomaterials containing ionic molecules, and beverages and foods containing alcohol molecules.

As the concentration of NaCl and alcohol molecules in the solution increases, the impedance (admittance) of the solution at 3300 MHz differs from the reference impedance of 50 Ω (0.02 S), and $S_{11}$ increases, resulting in an increase in Pwr and a decrease in EVM. The aqueous solution is considered an equivalent electrical passive circuit element, and an increase in the reflection coefficient $|S_{11}|$ does not increase the error vector, so the EVM value decreases.

Since the $S_{11}$ of the aqueous solution depends on the resonance caused by the rotation and vibration of the polar water molecule $H_2O$ and cluster, $S_{11}$ and Pwr become smaller as the concentration of $H_2O$ increases. The reflection characteristics of digital wireless signals from aqueous solutions highly depend on the amount of polarized molecular $H_2O$. The EVM value increases the symbol-clock error in the wireless signal transmission system. This study also clarified the relationship between the reflection of digital wireless signals, chemical materials, and biomaterials containing ionic molecules, and beverages and foods containing alcohol molecules.

## REFERENCE


[1] M. Grossi, B. Ricco, "Electrical impedance spectroscopy (EIS) for biological analysis and food characterization: a review," Journal of Sensors and Sensor Systems, 6: 303-325, 2017. https://doi.org/10.5194/jsss-6-303-2017

[2] M. Hussain, M, A. E. Keblawy, N. Akhtar, A. S. Elwakil, "Electrical Impedance Spectroscopy in Plant Biology," Sustainable Agriculture Reviews, 52: 395-416, 2021. https://link.springer.com/chapter/10.1007/978-3-030-73245-5 12.

[3] K. Kadan-Jamal, M. Sophocleous, A. Jogc, D. Desagani, O. Trog-Sussholz, J. Georgiou, A. Avni, Y. Shacham-Diamanda, "Electrical impedance spectroscopy of plant cells in aqueous buffer media over a wide frequency range of 4 Hz to 20 GHz," MethodsX, 8: 1-10, 2021. https://doi.org/10.1016/j.bios.2020.112485.

[4] M. V. Haeverbeke, B. D. Baets, B. D. Bernard, M Stock, "Plant impedance spectroscopy: a review of modeling approaches and applications," REVIEW article Sec. Plant Biophysics and Modeling, Front. Plant Sci., 14, 2023. https://www.frontiersin.org/journals/plant-science/articles/10.3389/ fpls.2023.1187573/full.

[5] L. F. Lima, A. L. Vieira, H. Mukai, C. M. G. Andrade, P.R. G. Fernandes, "Electric impedance of aqueous KCl and NaCl solutions: Salt con- centration dependence on components of the equivalent electric circuit," Journal of Molecular Liquids, 241: 530-539, 2017. https://doi.org/10.1016/j.molliq.2017.06.069.

[6] C. S. Widodo, H.S. Sela, D. R Santosa, "The Effect of NaCl Concentration on the Ionic NaCl Solutions Electrical Impedance Value using Electrochemical Impedance Spectroscopy Methods," The 8th Annual Basic Science International Conference, AIP Conf. Proc., 05003: 1- 6, 2021. https://doi.org/10. 1063/1.5062753.

[7] J. Slay, R. Sotner, T. J. Freeborn, J. Jerabek, L. Polak, J. Petrzela, "Distinguishing Liquid Solutions with Alcohol Using Electrical Impedance Measurements: Preliminary Study for Food Safety Applications," IEEE Sensors Journal, 23(22): 26997-27007, 2023. https://doi.org/10.1109/JSEN. 2023.3315798.

[8] A. Leo, G. A. Monteduro, S. Rizzato, A. Milone, G. Maruccio, "Miniaturized Sensors for Detection of Ethanol in Water Based on Electrical Impedance Spectroscopy and Resonant Perturbation Method-A Comparative Study," Sensor, 22(7): 2742. 2022. https://doi.org/10.3390/s22072742.

[9] K. Chinen, I. Kinjo, "Two-port Equivalent Circuit Deduced from S- parameter Measurements of NaCl Solutions," IETE Journal of Research. 877(3): 1-9, 2022. https://doi.org/10.1080/03772063.2022.2081264.

[10] K. Chinen, S. Nakamoto, I. Kinjo, "Alcohol Solutions Impedance and Equivalent Circuits," International Journal of Electrical and Computer Engineering Research, 4(2): 1-7, 2024. https://doi.org/10.53375/ijecer.2023.342.

[11] K. Chinen, S. Nakamoto, I. Kinjo, "RF Analysis of Fruit and Vegetables using Equivalent Circuits Deduced from S-parameters," International Journal of Electrical and Computer Engineering Research, 3(2): 18-24, 2024. https://doi.org/10.53375/ijecer.2023.342

[12] K. Chinen, S. Nakamoto, I. Kinjo, "Relationship Between Impedance Transition Point and Cell Wall in Plant Tissue," Quest Journals, Journal of Electronics and Communication Engineering Research, 10(3): 9-18, 2024. https://www. questjournals.org/jecer/papers/vol10-issue3/10030918.pdf.

[13] K. Chinen, S. Nakamoto, I. Kinjo, "Plant Cell Vacuolar Impedance and Equivalent Circuit," IOSR Journal of Electronics and Communication Engineering (IOSR-JECE), 19(3): 74-80, 2024. https://www.iosrjournals.org/iosr-jece/papers/ Vol.%2019%20Issue%203/Ser-1/D1903011826.pdf.

[14] P. Kumar, A. Kumari, "BER Analysis of BPSK, QPSK, 16-QAM & 64- QAM Based OFDM System Over Rayleigh Fading Channel," IOSR Journal of Electronics and Communication Engineering (IOSR-JECE), 11(4): 66-74, 2016. https://doi.org/10.9790/2834-1104036674.

[15] N5230A(VNA), https://www.keysight.com/us/en/product/N5230A/2port-pnal-series.html.

[16] E4438C(VSG), https://www.keysight.com/us/en/assets/7018-01039/data-sheets-archived/ 5988-4039.pdf.

[17] 89600S(VSA), https://www.keysight.com/us/en/products/software/pathwave-test-software/ 89600-vsa-software.html

[18] G. Rani, V. Chawla, "A Novel Study on Uplink and Downlink Transceivers for LTE System," International Advanced Research Journal in Science, Engineering and Technology, 3(12): 114-120, 2016. https://www.iarjset.com/ upload/2016/december-16/IARJSET%2021.pdf.

[19] AWR Design Environment Platform https://www.cadence.com/en US/home/tools/system-analysis/ rf-microwave-design/awr-design-environment-platform.html

[20] K. Chinen, I. Kinjo, "A 3.5 GHz Band RF Wireless Signal Transmission Mechanism in Various Aqueous Solutions," SSRG International Journal of Electrical and Electronics Engineering, 10(8): 102-111, 2023. https://doi.org/10.14445/ 23488379/IJEEE-V10I8P110.

[21] Polarities of solvents. https://www.shodex.com/en/dc/06/0117.html. Top > Applications > Synthetic Polymers > Polarities of solvents